10th International LISA Symposium (LISAX) IOP Publishing
Journal of Physics: Conference Series **610** (2015) 012024 doi:10.1088/1742-6596/610/1/012024

Disentangling the magnetic force noise contribution in LISA Pathfinder

M Armano[a], H Audley[b], G Auger[c], J Baird[n], P Binetruy[c], M Born[b], D Bortoluzzi[d], N Brandt[e], A Bursi[t], M Caleno[f], A Cavalleri[g], A Cesarini[g], M Cruise[h], K Danzmann[b], I Diepholz[b], R Dolesi[g], N Dunbar[i], L Ferraioli[j], V Ferroni[g], E Fitzsimons[e], M Freschi[a], J Gallegos[a], C García Marirrodriga[f], R Gerndt[e], LI Gesa[k], F Gibert[k], D Giardini[j], R Giusteri[g], C Grimani[l], I Harrison[m], G Heinzel[b], M Hewitson[b], D Hollington[n], M Hueller[g], J Huesler[f], H Inchauspé[c], O Jennrich[f], P Jetzer[o], B Johlander[f], N Karnesis[k], B Kaune[b], N Korsakova[b], C Killow[p], I Lloro[k], R Maarschalkerweerd[m], S Madden[f], D Mance[j], V Martín[k], F Martin-Porqueras[a], I Mateos[k], P McNamara[f], J Mendes[m], L Mendes[a], A Moroni[t], M Nofrarias[k], S Paczkowski[b], M Perreur-Lloyd[p], A Petiteau[c], P Pivato[g], E Plagnol[c], P Prat[c], U Ragnit[f], J Ramos-Castro[qr], J Reiche[b], J A Romera Perez[f], D Robertson[p], H Rozemeijer[f], G Russano[g], P Sarra[t], A Schleicher[e], J Slutsky[s], C F Sopuerta[k], T Sumner[n], D Texier[a], J Thorpe[s], C Trenkel[i], H B Tu[g], S Vitale[g], G Wanner[b], H Ward[p], S Waschke[n], P Wass[n], D Wealthy[i], S Wen[g], W Weber[g], A Wittchen[b], C Zanoni[d], T Ziegler[e], P Zweifel[j]

[a] European Space Astronomy Centre, European Space Agency, Villanueva de la Cañada, 28692 Madrid, Spain
[b] Albert-Einstein-Institut, Max-Planck-Institut für Gravitationsphysik und Universität Hannover, 30167 Hannover, Germany
[c] APC UMR7164, Université Paris Diderot, Paris, France
[d] Department of Industrial Engineering, University of Trento, via Sommarive 9, 38123 Trento, and Trento Institute for Fundamental Physics and Application / INFN
[e] Airbus Defence and Space, Claude-Dornier-Strasse, 88090 Immenstaad, Germany
[f] European Space Technology Centre, European Space Agency, Keplerlaan 1, 2200 AG Noordwijk, The Netherlands
[g] Dipartimento di Fisica, Università di Trento and Trento Institute for Fundamental Physics and Application / INFN, 38123 Povo, Trento, Italy
[h] Department of Physics and Astronomy, University of Birmingham, Birmingham, UK
[i] Airbus Defence and Space, Gunnels Wood Road, Stevenage, Hertfordshire, SG1 2AS, UK
[j] Institut für Geophysik, ETH Zürich, Sonneggstrasse 5, CH-8092, Zürich, Switzerland
[k] Institut de Ciències de l'Espai (CSIC-IEEC), Campus UAB, Facultat de Ciències, 08193 Bellaterra, Spain
[l] Istituto di Fisica, Università degli Studi di Urbino/ INFN Urbino (PU), Italy
[m] European Space Operations Centre, European Space Agency, 64293 Darmstadt, Germany
[n] The Blackett Laboratory, Imperial College London, UK
[o] Physik Institut, Universität Zürich, Winterthurerstrasse 190, CH-8057 Zürich, Switzerland
[p] SUPA, Institute for Gravitational Research, School of Physics and Astronomy, University of Glasgow, Glasgow, G12 8QQ, UK

[q] Department d'Enginyeria Electrònica, Universitat Politècnica de Catalunya, 08034 Barcelona, Spain
[r] Institut d'Estudis Espacials de Catalunya (IEEC), C/ Gran Capità 2-4, 08034 Barcelona, Spain
[s] NASA Goddard Space Flight Center, 8800 Greenbelt Road, Greenbelt, MD 20771, USA
[t] CGS S.p.A, Compagnia Generale per lo Spazio, Via Gallarate, 150 - 20151 Milano, Italy

E-mail: nofrarias@ice.cat

Abstract. Magnetically-induced forces on the inertial masses on-board LISA Pathfinder are expected to be one of the dominant contributions to the mission noise budget, accounting for up to 40%. The origin of this disturbance is the coupling of the residual magnetization and susceptibility of the test masses with the environmental magnetic field. In order to fully understand this important part of the noise model, a set of coils and magnetometers are integrated as a part of the diagnostics subsystem. During operations a sequence of magnetic excitations will be applied to precisely determine the coupling of the magnetic environment to the test mass displacement using the on-board magnetometers. Since no direct measurement of the magnetic field in the test mass position will be available, an extrapolation of the magnetic measurements to the test mass position will be carried out as a part of the data analysis activities. In this paper we show the first results on the magnetic experiments during an end-to-end LISA Pathfinder simulation, and we describe the methods under development to map the magnetic field on-board.

1. Introduction

LISA Pathfinder (LPF) [1] will test key technologies required for gravitational wave detection in space. The main goal of the mission is to achieve a residual differential acceleration noise between two free-falling test masses of $3 \times 10^{-14}\,\mathrm{m/s^2/\sqrt{Hz}}$ in the $1\,\mathrm{mHz} \leq \mathrm{f} \leq 30\,\mathrm{mHz}$ frequency band, expressed in terms of noise spectral density. The satellite is equipped with the Gravitational Reference Sensor [2] hosting the test mass and controlling its position inside the spacecraft through the so called drag-free control loop, and the Optical Metrology Subsystem [3] achieving pico-meter sensitivities in the measurement of the relative displacement of the test masses.

An equally important goal of the LPF mission is to disentangle the different contributions in the measured noise. Indeed, future space gravitational wave observatories [4] will benefit from the detailed noise model that LPF will provide. With that aim, the Diagnostic Subsystem [5] contains sensors and actuators to perform experiments during flight operations.

The rationale behind these experiments is to induce a high signal-to-noise ratio calibration signal that allows a good estimate of the coupling between the system and the perturbation under study. Once the calibration signal is off, we will use the derived coupling to estimate the level of noise induced in the main measurement by the perturbation. For the magnetic case, this means that a set of coils will induce a controlled magnetic field in the test mass volume, resulting in a force that will enable determining the magnetic properties of the test mass. These will be used to compute the force noise contribution due to the background magnetic field.

The tri-axial fluxgate magnetometers used in LPF are located far from the test mass due to the electromagnetic fields they emit, hence a precise interpolation is required in order to know the background magnetic field affecting the test masses. Hence, there are two different problems that need to be addressed to characterise the magnetic contribution to the total force noise budget:

- To estimate the magnetic parameters of the test mass through the observed response to an injected magnetic signal.
- To interpolate the measured magnetic field at the magnetometers to the position of the test masses.

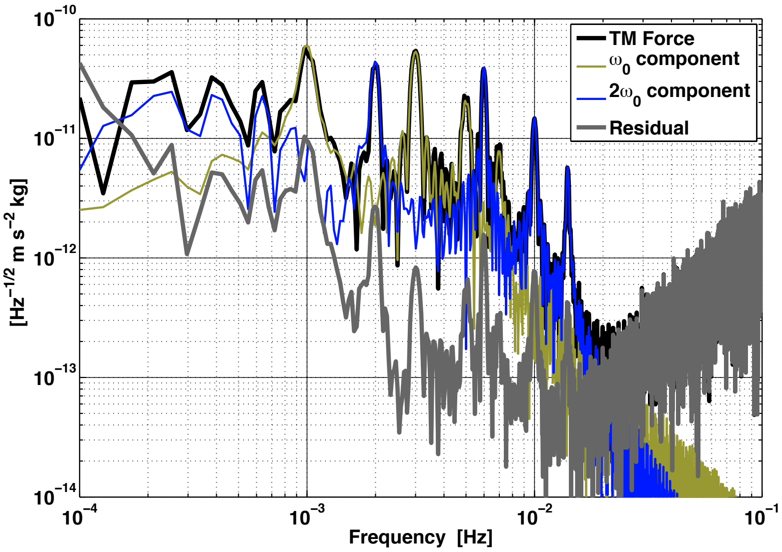

Figure 1. Reconstruction of the force in the x direction during the magnetic experiment in 4th operational exercise.

In the following we report on the latest developments for both

2. Estimation of test mass magnetic parameters

The inertial sensors displacement sensitivity at low frequencies is limited by actuation noise. After this, the main contribution limiting the sensor is due to the coupling of the test mass motion with background magnetic fields, which could represent up to 40% of the overall force noise budget. Although this coupling is greatly reduced because of the magnetic properties of the Au/Pt alloy from which the test mass is built, there is still a small remnant that needs to be taken into account.

If we assume an homogenous and isotropic test mass, the problem can be reduced to the estimation of the moment vector, $\vec{M} = (M_x, M_y, M_z)$, and susceptibility, $\chi = \chi_0 + i\,\chi_e$, in the following system of linear equations [6]

$$\begin{aligned} F_x &= \chi_0\, f_{DC} + M_x\, f_{x_{1\omega 0}} + \chi_0\, f_{x_{2\omega 0}} + \chi_e\, f''_{x_{2\omega 0}} \\ N_y &= M_z\, n_{y_{1\omega 0}} \\ N_z &= M_y\, n_{z_{1\omega 0}} \end{aligned} \tag{1}$$

where $f_{x_{1\omega 0}}$ is a force term at the injected frequency, ω_0; $f_{x_{2\omega 0}}$ is a force term at $2\,\omega_0$ and $f''_{x_{2\omega 0}}$ is a force term at $2\,\omega_0$ but out of phase when compared with the injected signal. All these terms depend on the magnetic field and the magnetic field gradient in the test mass volume and hence, are computed numerically and assumed known. The same applies to $n_{y_{1\omega 0}}$ and $n_{z_{1\omega 0}}$ which correspond to torques around the y and z axes due to the applied magnetic field.

This test mass characterisation scheme was put into test during the 4th operational exercise, which took place in November 2013. During this simulation, the science team was divided into small groups, each in charge of a different experiment. These simulations train the team for in-flight operations, so the data is received and processed in a mission-like scenario in terms of scheduling, satellite commanding and telemetry reception. In this occasion, the magnetic characterisation of the test took 19 h where the coil was commanded to apply a sinusoidal field

Table 1. Test mass magnetic parameters obtained during the 4th operational exercise.

Parameter	Value
χ_0	$(5.81 \pm 0.09) \times 10^{-5}$
M_x [Am^{-1}]	$(1.18 \pm 0.01) \times 10^{-4}$
M_y [Am^{-1}]	$(1.29 \pm 0.02) \times 10^{-4}$
M_z [Am^{-1}]	$(1.40 \pm 0.03) \times 10^{-4}$

injection at 1, 3, 5, and 7 mHz commanding in each case a 1 mA current into the coils. The set of frequencies is selected to maximize the SNR of the response signal [6].

The telemetry obtained during the simulation was processed using the LTPDA [7] magnetic data analysis pipeline. The main steps implemented in this procedure can be summarised as (1) pre-processing the data to detect possible irregularities as, for instance, missing data packets, (2) to translate the measured test mass displacement into measured force, based on the system dynamic parameters, (3) to compute the magnetic field at the test mass position based on the geometry of the problem and the applied current, (4) to compute the force contribution at the relevant frequencies in order to (5) solve the linear system of equations in Eq. (1).

The result of the experiment, shown in Fig. 1, is a clear signal when measuring the applied force on the test mass. The plot shows as well that the pipeline was able to retrieve the magnetic parameters characterising the test mass and reconstruct the applied force. Table 1 shows the values obtained by the pipeline. Notice that the imaginary part of the susceptibility was not estimated because this feature was not implemented in the simulator at the time of the simulation.

3. Magnetic field interpolation

The feed-back field from the tri-axial fluxgate magnetometers requires that they be located far from the desired measurement location. Although there exist proposals to alleviate the problem in future designs [8], the situation in LPF calls for a precise interpolation process. Several techniques have been proposed, among them the most promising is the usage of neural network algorithms [9] which learn from a set of given magnetic field configurations to interpolate the field in the real case.

Since the number of sources in the satellite greatly exceeds the number of available magnetometers, the interpolation becomes a degenerate problem. In all proposed methods the interpolation is usually strongly dependent on the *a priori* knowledge of the sources and therefore a clear detailed analysis of the distribution of the magnetic sources in the satellite is necessary for a successful analysis.

In Figure 2 we show the latest update on the distribution of magnetic sources in LISA Pathfinder. The figure graphically describes the complexity of the magnetic field due to the diversity of sources around the main experiment, located here in the position of the two test masses. It is important to notice that the recent replacement of the the field-emission electric propulsion (FEEP) thrusters by the cold gas ones has an important impact in the magnetic environment of the satellite. Indeed, the three main structures in Figure 2 are due to the cold gas latch valves (CGLV).

Again, this recent change stresses the importance of a good characterization on the ground. In Figure 3 we report a first study to evaluate the contributions of each identified magnetic source to the measured magnetic field for each magnetometer. These estimates show that the CGLV units are enough to explain nearly 60% of the contribution as measured for some magnetometers.

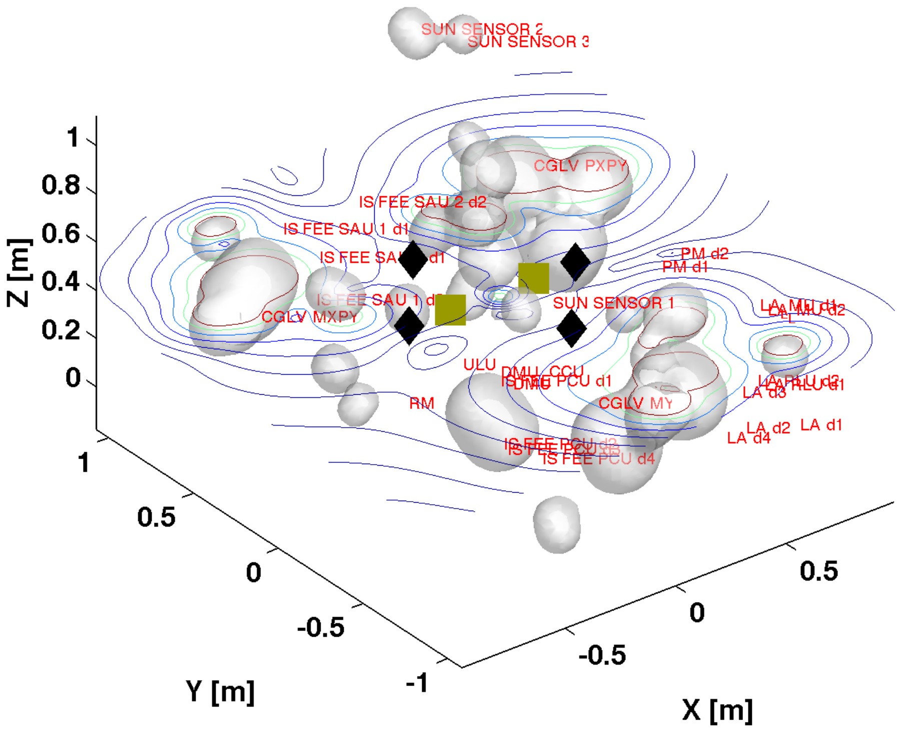

Figure 2. A magnetic map of LISA Pathfinder with some of the main magnetically active components. The shaded shapes show iso-surfaces of magnetic field while the contour lines display the magnetic field distribution in the XY plane defined by the test masses. The masses are shown as cubes in the center, the magnetometers appear as rhombus. Some of the acronyms in the plot are: cold gas latch valves (CGLV), phasemeter (PM), laser assembly (LA), radiation monitor (RM), ultraviolet lamp unit (ULU) and inertial sensor front-end electronics sensing and acutuation unit (IS FEE SAU)

Apart from these, each sensor is more sensitive to a given set of magnetic sources which explains the remaining contributions of the magnetic field.

As previously stated, *a priori* knowledge is crucial to solve the magnetic interpolation process. Hence, the ground characterisation of the units will be a valuable input for the in-flight characterisation since it will allow to exploit the particular spatial distribution of the magnetic sources in the LPF to help better characterise the magnetic field map on board.

4. Conclusions

Magnetically induced forces on the LISA Pathfinder test masses will be an important contribution to the final mission noise budget. Understanding the magnetic environment on board and characterising the magnetic properties of the test mass is crucial for the mission. During the 4th operational exercise, the experiments to induce a magnetic signal and thereby measure the magnetic moment and susceptibility of the test masses were simulated and the data analysis pipeline successfully tested, providing a successful characterisation.

The interpolation of the magnetic field from the magnetometers to the test mass position is

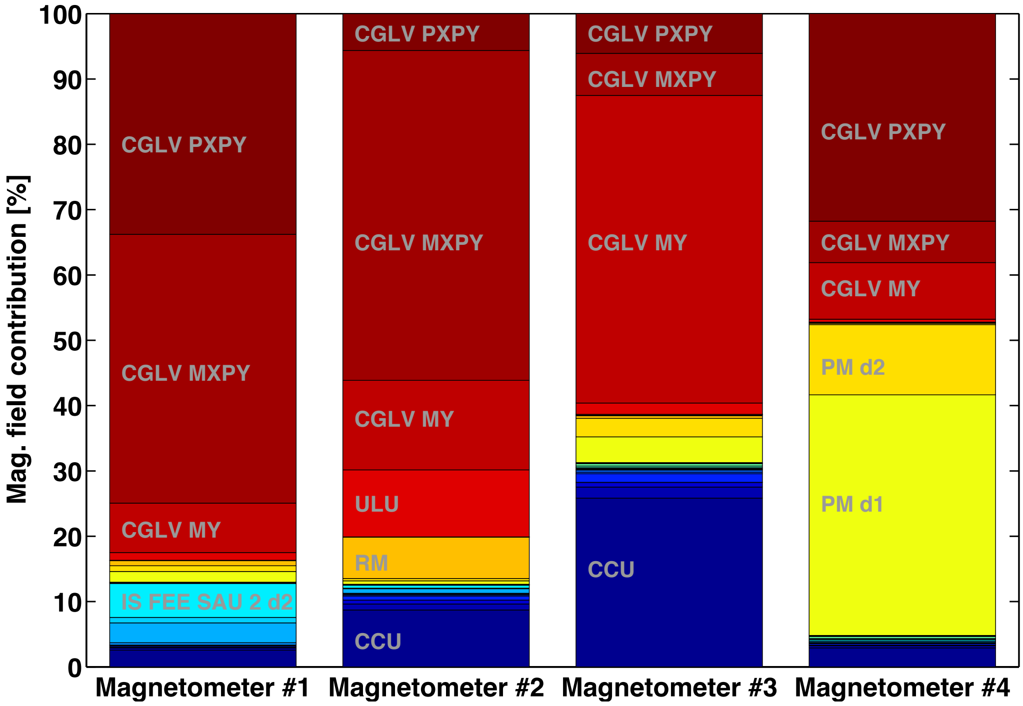

Figure 3. Main contributions to the total measured magnetic field in each magnetometer. The cold gas valve is dominating in each magnetometer.

a difficult task given the distribution of magnetic sources in the satellite surrounding the test masses. We have reported a first characterisation of the impact of individual magnetically active components to the total measured magnetic field. This information will be a valuable input for the interpolation methods being proposed, which relay on *a priori* knowledge of the magnetic field in the satellite.

References

[1] Antonucci F et al 2012, The LISA Pathfinder mission *Classical and Quantum Gravity* **29**, 124014
[2] Bortoluzzi D *et al.* 2003 Testing LISA drag-free control with the LISA technology package flight experiment *Class. Quantum Grav.* **20**, S89
[3] Heinzel G *et al.* 2005, Successful testing of the LISA Technology Package (LTP) interferometer engineering model *Classical and Quantum Gravity* **22**, S149
[4] Amaro-Seoane P *et al.* 2013, *The Gravitational Universe*, *Preprint* arXiv:1305.5720
[5] Lobo A *et al.* 2006 Inflight Diagnostics in LISA Pathfinder *AIP Conf. Proc.* **873**, 522
[6] Diaz-Aguiló M et al 2012, Inflight magnetic characterization of the test masses onboard LISA Pathfinder *Phys. Rev. D* **85**, 042004
[7] Hewitson M *et al.* 2009 Data analysis for the LISA Technology Package, *Class. Quantum Grav.* **26** 094003
[8] Mateos I *et al.* 2012, Temperature coefficient improvement for low noise magnetic measurements in LISA *Journal of Physics: Conference Series* **363**, 012051
[9] Diaz-Aguiló M *et al.* 2011, Neural network interpolation of the magnetic field for the LISA Pathfinder Diagnostics Subsystem *Experimental Astronomy* **30**, 1